Rev.Adv.Mater.Sci. 23(2010) 1-7

MAGNETIC PROPERTIES OF $LiNbO_3$ SINGLE CRYSTALS WEAKLY DOPED BY Yb AND/OR CODOPED BY Pr

T. Bodziony[1], S. M. Kaczmarek[1] and R. Kruk[2]

[1]Institute of Physics, West Pomeranian University of Technology, 70-310 Szczecin, Al. Piastów 17, Poland
[2]Institute of Nanotechnology, Forschungszentrum Karlsruhe GmbH, P.O. Box 3640, D-76021 Karlsruhe, Germany

Received: December 10, 2009

Abstract. The results of magnetic susceptibility measurements of weakly doped lithium niobate $LiNbO_3$: Yb (1 wt.%) and $LiNbO_3$: Yb (0.8 wt.%), Pr (0.1 wt.%) single crystals are reported for the first time. The dependence of magnetic susceptibility versus temperature fulfills the Curie – Weiss law. The estimated Curie – Weiss parameter is equal to $\Theta = -1.1 \pm 0.1$K and $\theta = -0.12 \pm 0.01$K for $LiNbO_3$: Yb and $LiNbO_3$: Yb, Pr, respectively. The magnetic susceptibility measurements confirm the presence of antiferromagnetic interactions between Yb^{3+} ions in weakly doped $LiNbO_3$: Yb, and $LiNbO_3$: Yb, Pr single crystals. The results of the magnetic susceptibility measurements emphasize an important role of a codopant in the magnetic properties of the main ytterbium impurity in a lithium niobate host lattice.

1. INTRODUCTION

Lithium niobate $LiNbO_3$ (LN) is one of the most studied ferroelectric and electro-optic materials [1-3]. An ideal LN lattice has two LN molecules in a rhombohedral unit cell with the lattice constants (at 296K) a = 0.514829 nm and c = 1.38631 nm [4,5]. The space group of an LN crystal is trigonal: $R3c$ (C_{3v}^6). LN is usually grown from congruent melt compositions with Li^+ to Nb^{5+} concentration ratio of the order of 0.945 ($x_c \approx 48.6\%$) giving rise to Li-deficient crystals that need intrinsic defects to satisfy the overall charge compensation. Various crystallographically non-equivalent centers may occur for a given RE^{3+} dopant ion, whereas the relative concentration of such centers depends on the stoichiometry (i.e. the Li/Nb concentration ratio). LN doped with an ytterbium (LN: Yb) single crystal has been the subject of many studies, e. g. Burns *et al.* [6] and Bonardi *et al.* [7]. Dong *et al.* [8] have studied the spin Hamiltonian (SH) parameters of Yb^{3+} ions in LN: Yb^{3+}, Mg^{2+} single crystals theoretically. The results of the [4-6] studies indicate that the site symmetry of Yb^{3+} centers in LN is C_3 and rare-earth (RE) ions occupy mainly the Li^+ sites. In case of LN: Mg, Yb, Dong [8] *et al.* have found that the Yb^{3+} ions may also occupy Nb^{5+} sites due to the MgO co-dopant influence. Choh *et al.* [9] come to a similar conclusion for Er^{3+} in Er and Mg co-doped LN single crystals. Montoya *et al.* [10] have provided evidence of the presence of Yb^{3+} pairs in an LN matrix. Montoya *et al.* [11] have also proposed a model for Yb^{3+} ions distribution in LN: Yb, Mg in which a fraction of dopant ions (about 10.4 % of all Yb^{3+} ions) forms pairs with one Yb^{3+} ion placed at the Li^+ site and another one at the Nb^{5+} site, while the rest of the Yb^{3+} ions are randomly distributed over the Li^+ sites.

Our previous studies were focused on spectroscopic investigations of LN: Yb [12,13] and LN: Yb, Pr single crystals [14,15]. We observed several paramagnetic centers originating both from isolated Yb^{3+} and interacting Yb^{3+} ions in both crystals. These paramagnetic centers showed low C_1 symmetry. The temperature dependence of the EPR

Corresponding author: T. Bodziony, e-mail: tbodziony@zut.edu.pl

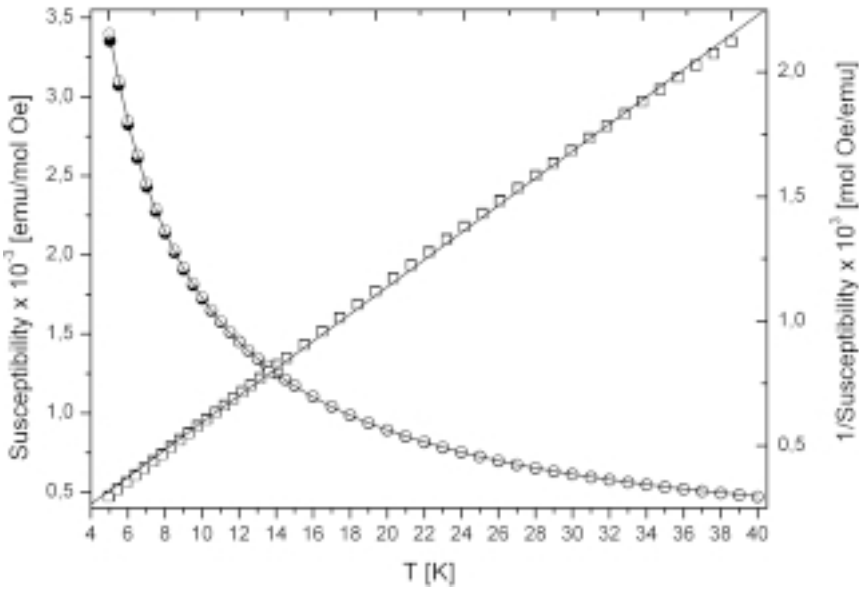

Fig. 1. The temperature dependence of MS (solid and empty circles, left scale) and inverse MS (solid and empty squares, right scale) for $LiNbO_3$: Yb (1 wt.%) in ZFC, (solid circles and squares) and FC (empty circles and squares) regimes with curves fitted according to the Curie – Weiss law.

line intensity and inverse line intensity confirmed the presence of interacting Yb^{3+} ions in addition to isolated Yb^{3+} ions in both crystals. The EPR line intensity fulfilled the Curie – Weiss law and yielded the antiferromagnetic interaction constant Θ = -0.6 ± 0.3K and ferromagnetic interaction constants Θ = 2.4 ± 0.1K for $LiNbO_3$: Yb and $LiNbO_3$: Yb, Pr samples, respectively [14]. We concluded that the presence of a Pr co-dopant forced substitution of the Yb^{3+} ions in the host crystal at sites other than Li and changed the interaction between Yb ions from the antiferromagnetic to a ferromagnetic one [14]. It should be emphasized that our earlier analyses of the EPR spectra and the investigation of the temperature behavior of the EPR lines intensity for $LiNbO_3$:Yb and $LiNbO_3$:Yb, Pr single crystals were based on the assumption of the existence of Yb^{3+} – Yb^{3+} pairs in a unit cell. Based on this indication, the isotropic exchange parameter J_{ex} was established and used to identify the positions of Yb^{3+} – Yb^{3+} dissimilar pairs in a unit cell of an $LiNbO_3$: Yb single crystal [15]. It was a simple assumption to take into account a small number of the dopant ions presented in both weakly doped lithium niobate single crystals.

In the present paper we are looking for additional evidence for the presence of Yb^{3+} ion pairs or more general, interacting Yb^{3+} ions in LN: Yb and LN: Yb, Pr single crystals using magnetic susceptibility (MS) measurements. It should be noticed that we have found only one paper partially devoted to magnetic measurements of LN. J. Diaz-Caro *et al.* [16] have studied optical and magnetic properties of the LN:Cr, Mg crystal and stressed the importance of MgO concentration.

The paper consists of three parts: first, the material and the methods are briefly described. Next, the results of the new magnetic measurements of weakly doped $LiNbO_3$: Yb (1 wt.%) and $LiNbO_3$: Yb (0.8 wt.%), Pr (0.1 wt.%) single crystals are presented. At the end, the results obtained from the EPR and MS measurements are compared.

2. EXPERIMENTAL

LN doped with 1 wt.% of Yb^{3+} and LN doped with 0.8 wt.% of Yb^{3+} and simultaneously codoped with 0.1 wt.% of Pr single crystals were grown along the ***c***-axis from congruent melt by the Czochralski method in the Institute of Electronic Materials Technology. A more detailed description of the applied growth process was presented elsewhere [17].

EPR spectra were recorded using a Bruker E 500 X-band spectrometer (ν ~ 9.4 GHz) with 100 kHz field modulation equipped with an Oxford flow cryostat for measurements at temperatures from the liquid nitrogen temperature down to 4K. Mag-

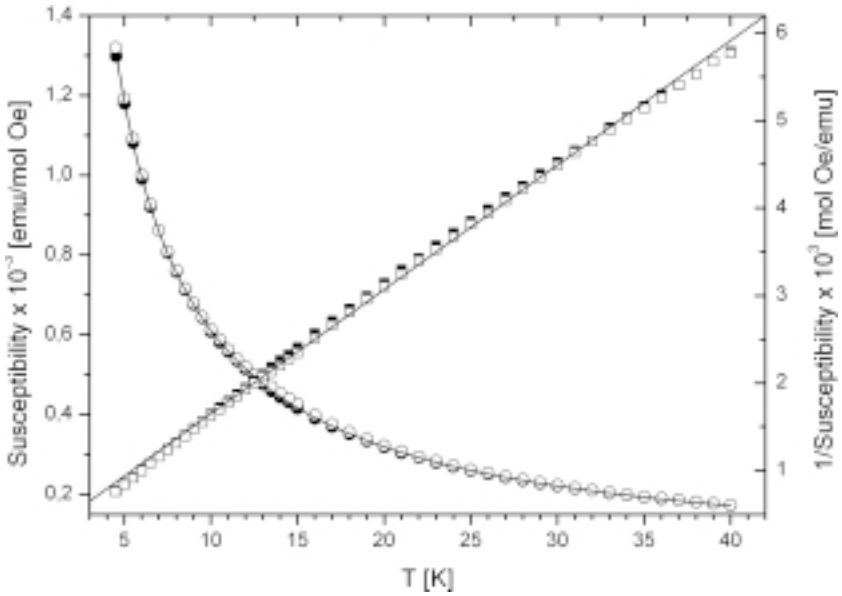

Fig. 2. The temperature dependence of MS (solid and empty circles, left scale) and inverse MS (solid and empty squares, right scale) of $LiNbO_3$: Yb (0.8 wt.%), Pr (0.1 wt.%) in ZFC (solid circles and squares) and FC (empty circles and squares) regimes with curves fitted according to the Curie – Weiss law.

netic measurements were performed in the temperature range of 4 to 40K using a SQUID magnetometer. At first, the sample was cooled without a magnetic field (zero field cooling, ZFC) and the magnetic measurements were carried out with temperature increasing from 4K up to 40K with the applied field of 200 Oe. Next, the sample was cooled in a magnetic field of 200 Oe (field cooling, FC) to 4.5K and the magnetic measurements were carried out with the temperature increasing up to 40K in a magnetic field of 200 Oe. The direction of the magnetic field was parallel to the optical *z*-axis (crystallographical *c*-axis) of the LN unit cell. The mesurments were performed in the Institute of Nanotechnology, Karlsruhe, Germany.

3. MAGNETIC SUSCEPTIBILITY MEASUREMENTS

Fig. 1 shows the temperature dependence of MS and inverse MS (marked by solid circles and solid squares, respectively) measured in the ZFC and FC modes for an LN: Yb single crystal. In Figs. 1 and 2 the ZFC and FC points are marked by solid and empty squares or circles, respectively. Unfortunately, they are nearly superimposed onto each other. We have found that the measured MS follows the Curie – Weiss law, $\chi = a + C/(T - \theta)$, where a – a term responsible for the diamagnetic susceptibility. This law is plotted as solid lines in Fig. 1. It came as a surprise for us because the Curie law is suitable for isolated paramagnetic ions in a diamagnetic matrix. It should be noticed that the range of values of the MS measured for LN: Yb in the present study matches well with the susceptibility values obtained for the LN:Cr:MgO crystal by J. Diaz-Caro *et al.* [16]. The relatively higher value of the MS in our experiment indicates that a substantial portion of ytterbium ions was incorporated into the LN crystal lattice during the growth process. However, we used a different magnetic ion with a different magnetic moment (Yb^{3+} versus Cr^{3+}).

The MS and inverse MS dependences versus temperature measured for LN: Yb, Pr single crystal are presented in Fig. 2. The left hand side scale is attributed to the MS, while the right-hand side scale - to the inverse of MS. The ZFC (solid circles and squares) and FC (empty circles and squares) points are nearly superimposed onto each other as previously. The Curie – Weiss law is also plotted in Fig. 2 as a solid line and a solid curve.

It is necessary now to discuss the similarities and differences between the EPR integrated intensity, measured and published earlier, and the MS intensity for both the LN: Yb and LN: Yb, Pr samples [14,15]. The total intensity of the EPR spectra for LN: Yb and LN: Yb, Pr single crystals has been

computed by double integration of the EPR signal. When the temperature decreases, the total intensity of the EPR lines gradually increases, showing a sharp increase at about 7K followed by a strong or slight decrease with a temperature decrease below 7K for LN: Yb and LN, Yb, Pr single crystals, respectively. No analogous behavior is observed in the temperature dependence of the MS (see Fig. 1 and Fig. 2, solid circles, left scale). The MS measurements were finished at a temperature about 4K, being too high to observe a maximum and following a decrease in MS. This could be the main reason for the observed different behavior.

The temperature dependence of the inverse total intensity of the EPR spectra shows a linear increase with a temperature increase from 4K up to ~ 40K followed by a linear increase up to 65K, but with a different slope, clearly visible for LN: Yb [14,15]. Analogous behavior can be observed in the inverse of MS (see Figs. 1 and 2, solid squares, right scale). Of course, the slopes of the lines are different in case of both single crystals and in both kinds of measurements. The temperature dependence of the total intensity of the EPR spectra shows that the crystal codoped with praseodymium (LN: Yb, Pr) gives a much more intense EPR signal than that doped only with ytterbium (LN: Yb) in spite of the intentional concentration of Yb ions, which is lower by 0.2% in codoped LN than in LN doped only with ytterbium [15]. However, the scales on Figs. 1 and 2 reveal that MS is stronger in the case of the LN: Yb sample than for the codoped LN; Yb, Pr one. A full analysis of these differences is given in the next chapter.

4. DISCUSSION AND CONCLUSIONS

Generally, the temperature dependence of MS, χ, in a paramagnetic region can be written as [18]:

$$\chi = a + \frac{C_i}{T} + \frac{C_n}{T - \Theta}, \qquad (1)$$

where the three above terms account for the diamagnetic susceptibility, isolated paramagnetic ions and clusters, respectively. $C_i = n_i m_i^2/3k$, $C_n = n_n m_n^2/3k$ are Curie constants for isolated and clustered (or generally interacting) Yb ions, n_i and n_n are the numbers of isolated and interacting ions; m_i and m_n are the corresponding high-temperature ($T >> |\Theta|$) values of the magnetic moment, and Θ is the Curie - Weiss constant. J. Kliava *et al.* have applied the formula (1) to the description of Gd^{3+} clusters in multicomponent oxide glasses, where the gadolinium is added in quantities from 0.1 to 10 mass% [18].

In both measurements we have observed that the signal originating from interacting Yb^{3+} ions dominates in the low temperature region [15]. Therefore, we have used Eq. (1) to fit the temperature dependence of both the total intensity of the EPR spectra and the value of MS. The best fit was obtained when we ignored the second term in Eq. (1):

$$\chi = a + C / (T - \theta). \qquad (1a)$$

In case of the EPR measurements, the temperature dependence of the total inverse intensity of the EPR signal is well described by a linear approximation, e. g. by Eq. (1a), in the temperature range between 7.5K and 38K. This allows us to determine the Curie – Weiss constants θ = -0.6 ± 0.3K and θ = 2.4 ± 0.1K for LN: Yb and LN: Yb, Pr single crystals, respectively [14]. Next, we apply an effective spin Hamiltonian, which includes contributions from both isolated Yb^{3+} ions and magnetically coupled dissimilar Yb^{3+} ion pairs. We assumed the simple dipole – dipole magnetic interaction between Yb^{3+} – Yb^{3+} ions. Using it for the LN: Yb crystal, we were able to calculate the exchange interaction parameter J_{ex} = -0.0283(13) cm^{-1} [15]. The negative sign of J_{ex} indicates that the magnetic interactions within each Yb^{3+}-Yb^{3+} pair in the LN: Yb single crystal are of a antiferromagnetic nature.

In case of MS measurements it can be noticed that the measured MS obeys Eq. (1a) which is marked as a solid line and a solid curve in Figs. 1 and 2. The estimated parameters are equal to: θ = -1.1±0.1K and C = 0.019±0.01 [emu K/mol Oe] for LN: Yb (1.0 wt.%) sample. The negative value of the Curie - Weis constant, θ, suggests antiferromagnetic coupling between Yb^{3+} ions. The MS very well fulfils Eq. (1a) for LN: Yb, Pr, too (see Fig. 2). The estimated parameters are: θ = -0.12 ± 0.01K and C = 0.41 ± 0.01 [emu·K/mol Oe] for LN: Yb, Pr single crystal. The negative value of Curie – Weiss temperature, θ, suggests antiferromagnetic coupling between Yb^{3+} ions. The parameters of the Curie - Weiss temperature determined from MS and EPR measurements are gathered in Table 1 and Table 2 for LN: Yb and LN: Yb, Pr single crystals, respectively.

The exchange interaction energies have been estimated within molecular field (Weiss molecular field) approximation using the well known expression, e.g. being a part of the Curie-Weiss law [19]:

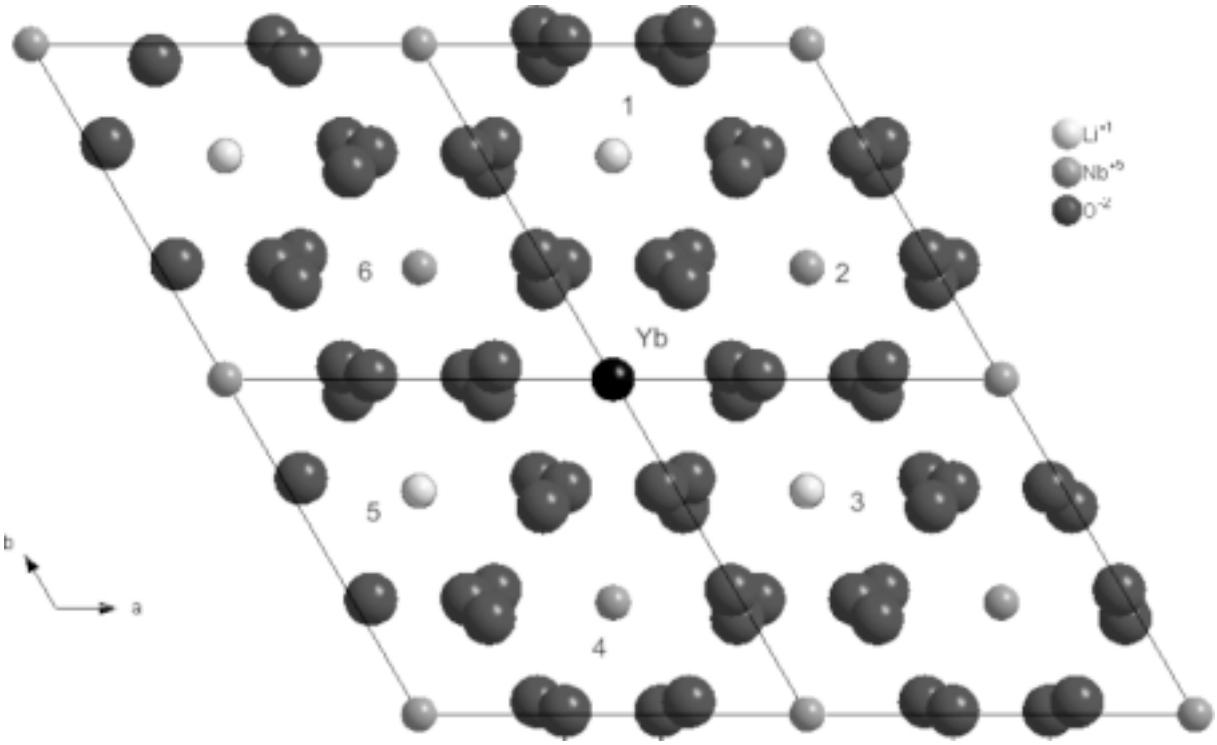

Fig. 3. Crystallographic arrangement of constituent atoms in LN: Yb crystal structure projected on the **ab** plane (0001 plane) perpendicular to the **c** – axis. The Yb^{3+} ion enters at the Nb^{5+} site (the black solid circle in the middle). 1, 3, 5 - Li^+ sites in the first shell "above" (light grey), 2, 4, 6 – Nb^{5+} sites (dark grey) in the first shell "below" the Yb^{3+} ion.

$$\theta = 2zJ_{ex}J(J+1)/3k, \qquad (2)$$

where J_{ex} – the exchange parameter, k – Boltzmann constant, J – total angular moment and z – is the number of magnetic ions surrounding the ytterbium ion. For 4f ions **S** is not a good quantum number, but the total angular momentum **J** is. The values of **S**, **L**, **J** are listed in many books. For Yb^{3+} ions (shell $4f^{13}$) we taken $S = S_{eff} = 1/2$, $L = 3$, $J = 7/2$ [20]. The resulting value of zJ_{ex} is: zJ_{ex}= -0.0728±0.0066 cm^{-1} and zJ_{ex}= -0.0079±0.0013cm^{-1} for LN: Yb and LN: Yb, Pr crystals, respectively. Now, we need to estimate the z value.

Fig. 3 shows the crystallographic arrangement of a constituent atom in the LN: Yb crystal structure projected on the **ab** plane (0001 plane) perpendicular to the **c** – axis. It is assumed that the Yb^{3+} ion enters at the Nb^{5+} site (shown in the middle of the structure). If the Yb^{3+} ion enters at Li^+, the picture is similar. The site numbers 1, 3, 5 – are Li^+ sites in the first shell "above" (light grey), while the sites numbers 2, 4, 6 – are Nb^{5+} sites (dark grey) in the first shell "below" the Yb^{3+} ion. There are six different sites of magnetic ions surrounding the Yb^{3+} ion in its first shell, so we put z = 6 to Eq. (3). Assuming that the number of nearest magnetic neighbors of an ytterbium ion is equal to z = 6, the approximate value of the exchange parameter J can be calculated. All values of zJ_{ex}, J_{ex} parameters, obtained from the MS (and EPR measurements) are collected in Tables 1 and 2. It should be mentioned that the value J of the exchange parameter for EPR measurements is the same for both crystals LN; Yb and LN: Yb, Pr [15].

It is interesting to compare the θ, C, zJ_{ex}, J_{ex} values obtained from the MS and EPR measurements for both the LN: Yb and LN: Yb, Pr samples. Table 1 shows that both the MS and EPR measurements give a Curie –Weiss constant with a negative sign and a quite similar value in case of the LN: Yb singe crystal. The absolute value of the exchange parameter J_{ex} is only about two times greater in case of the EPR than MS measurements. It can be seen in Table 2 that the Curie – Weiss constant is negative (and close to zero) and positive for MS and EPR measurements, respectively, in case of the LN: Yb, Pr single crystal.

Table 1. Curie temperature θ and constant *C* of the temperature dependence of MS and the EPR spectra total intensity for an $LiNbO_3$: Yb (1 wt.%) single crystal (z = 6).

	θ [K]	*C* [emu K/mol Oe]	zJ_{ex} [cm^{-1}]	J_{ex} [cm^{-1}]
MS	-1.1 ± 0.1	0.019 ± 0.001	-0.0728 ± 0.0066	-0.0121 ± 0.0011
EPR	-0.6 ± 0.3 [15]	-	-	-0.0283 ± 0.0013 [15]

Table 2. Curie temperature θ and constant *C* of the temperature dependence of MS and the EPR spectra total intensity for an $LiNbO_3$: Yb (0.8 wt.%), Pr (0.1 wt.%) single crystal (z = 6).

	θ [K]	*C* [emu K/mol Oe]	zJ_{ex} [cm^{-1}]	J_{ex} [cm^{-1}]
MS	-0.12 ± 0.1	0.41 ± 0.01	-0.0079 ± 0.0033	-0.0013 ± -0.0006
EPR	2.4 ± 0.1 [14]	-	-	-0.0283 ± 0.0013 [15]

The magnetic susceptibility measurements indicate that there are much more magnetic ions in the LN: Yb single crystal than in the LN: Yb, Pr sample. This conclusion agrees with intentional concentrations and is opposite to the EPR total intensity measurements of these two samples. The LN: Yb single crystal EPR spectrum is much less intense than the codoped one [15]. The EPR lines originate from a small fraction of paramagnetic ions, whereas in the MS measurements recorded signal originates from all paramagnetic species. A crucial role in understanding the above differences is played by the relaxation time between paramagnetic ions and a host crystal lattice suitable for the X – band EPR spectroscopy (~ 9.4 GHz) [21]. It means that a substantial part of the Yb^{3+} ions present in the host lattice may be not "visible" in the EPR spectra. The EPR total intensity for the LN: Yb sample is much lower than that of the codoped LN: Yb, Pr because the number of Yb ions, which can be visible in the EPR spectroscopy is much greater in the case of the codoped lithium niobate single crystal (LN: Yb, Pr) than in the Yb only doped sample. It clearly shows how important the codopant's presence in the LN crystal is, e.g. the praseodymium ions. Codopants significantly influence the behavior and crystallographic position of the main dopant in the lithium niobate crystal lattice, e.g. Yb ions. Finally, the presence of a codopant in a lithium niobate crystal, e.g. Pr ions, may explain the above mentioned difference between the EPR and MS measurements.

For the LN: Yb, Pr sample we have observed that the absolute value of the exchange parameter J_{ex} is about twenty times greater in case of the EPR than MS measurements. The presence of any codopant in the LN crystal structure, e.g. praseodymium ions, is crucial to explain it. The praseodymium ions (Pr^{3+}, shell $4f^2$) are non-kramers ions but have magnetic moment. It may explain above differences. Aditionally, the praseodymium ions facilitate substitution of ytterbium ions for constituent ions in the congruent LN crystal lattice and "enforce" ytterbium ions to choose only specific sites (see Fig. 3). As a result, the codopant ions change the character of the exchange interaction between Yb^{3+} ions from antiferromagnetic to ferromagnetic coupling, which is observed as a change of the Curie – Weiss parameter (see Tables 1 and 2, EPR measurement).

Finally, the results obtained from the MS measurements are an independent confirmation of the existence of an exchange interaction of Yb^{3+} ions in weakly doped LN single crystals. However, we could not simply tell that MS measurements confirm the existence of Yb^{3+} – Yb^{3+} pairs in an LN: Yb crystal. We can obtain an Yb^{3+} – Yb^{3+} pairs model of interaction if only one Yb^{3+} ion is present in the first shell (see Fig. 3). But generally speaking, much more of Yb^{3+} ions: 2, 3, up to 6 may be present in the first shell. In spite of the low intentional concentration of the Yb ions (1.0 wt. % and 0.8 wt. % for LN: Yb, and LN: Yb, Pr, respectively) the presence of Yb^{3+} ion clusters in a lithium niobate lattice could not be excluded. Any direct confirmation of the existence of Yb^{3+} – Yb^{3+} pairs in LN weakly doped with ytterbium needs further investigations. The results of the MS measurements emphasize also the important role of the codopant in the magnetic properties of the main, paramagnetic impurity in an LN lattice.

REFERENCES

[1] J. M. Cabrera, J. Olivares, M. Carrascosa, J. Ramis, R. Muller and E. Dieguez // *Advan. Phys*. **45** (1996) 349.
[2] H. E. Conzetti and S. I. Stepanov // *Rep. Prog. Phys.* **57** (1994) 39.
[3] *Properties of Lithium Niobate, 1989 Inspec* (EMIS Datareviews Series No. 5).
[4] S. C. Abrahams, J. M. Reddy and J. L. Bernstein // *J. Phys. Chem. Solids* **27** (1966) 997.
[5] G. Malovichko, V. Grachev, V. Kokanyan and O. Shirmer // *Phys. Rev. B* **59** (1999) 9113.
[6] G. Burns, D. F. O'Kane and R. S. Title // *Phys. Rev.* **167** (1968) 314.
[7] C. Bonardi, C. J. Magon, E.A. Vidoto, M. C. Terrile, L. E. Bausa, E. Montoya, D. Bravo, A. Martin and F. J. Lopez // *J. Alloy Comp.* **323—324** (2001) 340.
[8] H.-N. Dong, S.-Y. Wu and W.-C. Zheng // *J. Phys. Chem. Solids* **64** (2003) 695.
[9] S. H. Choh, J. H. Kim, I. W. Park, H. J. Kim, D. Choi and S. S. Kim // *Appl. Magn. Reson.* **24** (2003) 313.
[10] E. Montoya, O. Espeso and L. E. Bausa // *J. Lumin.* **87– 89** (2000) 1036.
[11] E. Montoya, L. E. Bausa, B. Schaudel and P. Goldner // *J. Chem. Phys.* **114** (2001) 3200.
[12] T. Bodziony and S.M. Kaczmarek // *Res. Chem. Intermed.* **33** (2007) 885.
[13] T. Bodziony and S.M. Kaczmarek // *Optical Materials* **29** (2007) 1440.
[14] T. Bodziony, S.M. Kaczmarek and J. Hanuza // *Journal of Alloys and Compounds* **451/1** (2008) 240.
[15] T. Bodziony, S.M. Kaczmarek and C. Rudowicz // *Physica B* **403** (2008) 207.
[16] J. Diaz-Caro, J. Garcia-Sole, J.L. Martinez, B. Henderson, F. Jaque and T.P.J. Han // *Optical Materials* **10** (1998) 69.
[17] I. Pracka, M. Malinowski, A. L. Bajor, B. Surma, Z. Gałązka, M. Swirkowicz and M. Możdżonek // *Proc. SPIE* **3178** (1997) 295.
[18] J. Kliava, A. Malakhovskii, I. Edelman, A. Potseluyko, E. Petrakovskaja, I. Bruckental, Y. Yeshurun and T. Zarubina // *Journal of Superconductivity and Novel Magnetism* **20,** DOI: 10.1007/s10948-006-0116-4.
[19] C. Kittel, *Introduction to Solid State Physics* (John Wiley & Son, 2005).
[20] C. Blundell, *Magnetism in Condensed Matter* (Oxford University Press, 2001).
[21] A. Abragam and B. Bleaney, *Electron paramagnetic resonance of Transition Ions* (Oxford, Clarendon Press,1970).